

Energy recovery through co-pyrolysis of wastewater sludge and forest residues – The transition from laboratory to pilot scale

Marzena Kwapinska^{a,*}, Alen Horvat^b, David A. Agar^c, James J. Leahy^d

^a Department of Chemical Sciences, University of Limerick, V94 T9PX, Ireland

^b Carlos III Univ Madrid, Energy Syst Engrn Grp, Thermal & Fluids Engrn Dept, Avda Univ 30, Madrid, 28911, Spain

^c Swedish Univ Agr Sci, Dept Forest Biomat & Technol, SE-90183, Umea, Sweden

^d Department of Chemical Sciences, Bernal Institute, University of Limerick, V94 T9PX, Ireland

ARTICLE INFO

Keywords:

Pyrolysis gas

Tar

Char

Thermal conversion

Circular economy

Gas impurities

ABSTRACT

Anaerobically digested sewage sludge mixed with forest residues was pyrolysed at 800 °C, at laboratory and pilot scale. The study quantified differences in char and gas yields for tests carried out in a simple fixed bed laboratory reactor and rotating retort pyrolyser at pilot scale, when the residence time of feedstock was 10 min in both cases. The yield of char from pilot scale was 4 % lower than from laboratory scale while the yield of gas was 15.7 % higher. During the pilot scale pyrolysis of anaerobically digested sewage sludge blended with forest residues the gas quality for energy recovery applications was assessed and the fate of impurities (tar, NH₃ and H₂S) was investigated. The raw pyrolysis gas contained 14.6 g/Nm³ of tar, 36.9 g/Nm³ of NH₃ and 793 ppm of H₂S. Sixteen N-containing tar species were identified of which pyridine, propenenitrile, 2-methyl-, benzonitrile, and indole are found to be the most abundant. The yield of N-containing tar compounds accounted for approx. 12 % of total tar content. Conditioned pyrolysis gas contained 7.1 g/Nm³ of tar, 0.036 g/Nm³ of NH₃ and 119 ppm of H₂S. Benzene was by far the most abundant tar compound followed by toluene and styrene. The specifications of the used internal combustion engine were exceeded due to the sum of tar compounds such as fluoranthrene and pyrene with 4+ aromatic rings (at 0.0015 g/Nm³) and NH₃ content. The effectiveness and sustainability of energy recovery in wastewater treatment can be improved using forest industry by-products.

1. Introduction

Societies are moving toward greater sustainable utilisation of resources and the development of more circular economies. Two important and widely represented sectors are municipal wastewater treatment and forestry. Activities in water and forest utilisation are closely linked to UN Sustainable Development Goals (SDGs) and EU climate objectives.

1.1. Sewage sludge

Wastewater treatment in Ireland generates some 59,000 tonnes (2017) of sludge (dry mass) and is forecast at 96,000 tonnes by 2040 [1]. Some 80 % is treated to produce biosolids, which are reused in agriculture through land spreading. EU legislation or Codes of Good Practice regulate the disposal of sludge in Member States [2]. The latter stipulates that concentrations of heavy metals (Zn, Cd, Cu, Cr, Hg, Ni, Pb), polychlorinated biphenyls, polychlorinated dibenzo-p-dioxins and

dibenzofurans and polycondensated aromatic hydrocarbons in addition to the concentration of macro and micro-nutrients have to be monitored annually [3]. However, biosolids contain other contaminants that are neither monitored nor regulated. Those that can occur in wastewater sludge and generate concern include metallic nanoparticles, toxic organic contaminants, micro-plastics, pathogenic bacteria and viruses [4–9]. Therefore, land spreading and the circular economic benefits of sludge reuse is under increasing scrutiny. Quality assurance schemes in food production have also reduced the incentive for land spreading of biosolids. Therefore, it is important to explore alternative outlets and potential for utilising wastewater sludge.

Anaerobic digestion (AD) of sewage sludge is a common treatment at wastewater treatment plants to produce biogas but the process cannot recover all the energy in sludge. Lignin is the most recalcitrant component and is a major barrier to the full conversion of biomass (including sludge) into biogas [10,11]. AD sludge is still energy rich and contains considerable organic matter, which is poor in biodegradability. AD

* Corresponding author.

E-mail address: Marzena.Kwapinska@ul.ie (M. Kwapinska).

<https://doi.org/10.1016/j.jaap.2021.105283>

Received 24 November 2020; Received in revised form 25 June 2021; Accepted 5 August 2021

Available online 8 August 2021

0165-2370/© 2021 The Authors. Published by Elsevier B.V. This is an open access article under the CC BY license (<http://creativecommons.org/licenses/by/4.0/>).

reduces also odours and pathogens, but the risks associated with hazardous substances contained in sludge, e.g. persistent organic pollutants, cannot be alleviated via AD, and the digested sludge would impact on the environment and on public health if necessary treatment is not implemented.

1.2. Thermal treatment

High-temperature thermal treatment of sewage sludge destroys organic pollutants through complete inertization, making it a promising environmentally friendly disposal [12–14]. Sludge incineration is the main alternative to land spreading, with 40 % of wastewater sludge in Europe being incinerated in 2015. Incineration enables volume and pollutant reduction, in addition to enrichment and recovery of phosphorus from ashes [15], but represents a net energy cost due to the absence of energy recovery. Alternative thermal treatment processes for sewage sludge include pyrolysis [12,13,16] and gasification [17].

1.3. Pyrolysis and benefits

Sewage sludge pyrolysis (degradation of organic matter under an inert atmosphere) has mainly been investigated at laboratory [18] or bench scale [19] with one demonstration scale process in Germany [14]. Pyrolysis product yields are affected by the process conditions including temperature, heating rate, residence time and feedstock properties [20]. Pyrolysis is an attractive sludge treatment technology because it can be deployed at relatively small scale at decentralised locations, which are typical of the wastewater treatment plants in Ireland. In its simplest configuration, a pyrolysis process can operate with a cracking unit to produce only a gaseous energy carrier and a char.

1.4. Sludge properties

Sewage sludge has a high moisture content, a high nitrogen concentration (the main plant nutrient present), a low carbon content (low heating value), a high ash content and contains several heavy metals [13]. After AD, sludge is typically more than 80 % (wet basis) water, even after de-watering (Personal communication with WWTP 2016; sludge after dewatering has 84 % water, 16 % solids).

The required energy input for pyrolysis can be partitioned into 1) the energy needed to remove water from the feedstock (i.e. drying) and 2) the calorific requirement of pyrolysis itself [21]. The high moisture content of sludge has a major impact on the choice of thermal treatment as the thermal energy required to remove water is subject to thermodynamics and is directly proportional to the amount of water [22]. It follows that sludge drying requires twice as much energy as a woody biomass, whose green moisture content is usually around 40 % [23]. Consequently, Kim and Parker report a drying energy of two to three times higher than the energy demand for pyrolysis (300–500 °C) itself [24]. In other words, drying can consume almost half of the energy content of the sludge [16].

The high nitrogen concentration can also be problematic in thermal treatment. Some fraction of the nitrogen is volatilized during pyrolysis, making post treatment scrubbing of the product gas or flue gas a necessity [16,25]. Woody biomass by comparison has a low nitrogen content.

1.5. Forest residues

Forestry operations generate forest residues, treetops and branches from timber harvesting. Forest residues are abundant in many EU states [26] and are widely used in combustion or as raw material for fuel pellets in Nordic countries [27]. Their availability in Ireland is about 1.3 million m³ annually [28] or roughly six times the amount of sludge generated. Significant environmental benefits justify the extraction and use of residues in thermal conversion processes [29,30]. As

small-diameter woody fractions they can have an as-received moisture content of 38–48 % (wet basis) due to natural drying in the forest [23]. Their high heating value (> 20 MJ kg⁻¹ dry mass), low nitrogen (< 0.5 % dry mass) and low ash (< 2 % dry mass) content complement the higher values for these properties in sewage sludge, making mixtures of sludge and forest residues interesting for bolstering the feedstock properties in pyrolysis.

1.6. Summary of other relevant pyrolysis studies using SS and/or forest residues

Pyrolysis of anaerobically digested sewage sludge in fluidized bed reactors has been reported by many authors [31–33] but their work has focused on maximizing the yield of liquid products. No published studies deal with slow pyrolysis of anaerobically digested sewage sludge for gas production. With the exception of one laboratory-scale study [34], the slow pyrolysis of forest residues (above 300 °C) at pilot-scale has not been previously reported.

One of the main concerns in all thermal conversion processes is the release of heavy metals and contaminants such as NH₃, HCl, HCN, H₂S [35–37]. It is a feature of slow pyrolysis at low temperature that heavy metals present in the feedstock remain mostly concentrated and immobilized in the char product [38,39]. The high mineral content in the char dilutes the fixed carbon content and [34] is not suitable as a reducing agent in metallurgical applications. Potential applications for the pyrolysis products, then depend largely on process parameters, on the presence of various contaminants [40] and these can be feedstock specific. For example, it has been reported that sewage sludge derived carbonaceous pyrolysis products can be used as fertilizer for P-deficient and toxic metal polluted soil [41].

Co-pyrolysis of sewage sludge with other biomass such as saw dust, rice straw, cotton stalks, hazelnut shells and willow has been studied [42–46] but focused mainly on char properties. Co-pyrolysis of sewage sludge with biomass dilutes inorganic matter content and toxic compounds present in sewage sludge [42,47]. It also improves other physicochemical properties of produced chars [48,49] and facilitates transformation of metals into more stable forms [43,46].

1.7. Purpose of study

This study investigates slow pyrolysis of sewage sludge and forest residues as a conversion technology for energy recovery. The three main objectives are 1) to compare laboratory and pilot scale pyrolysis processes when different modes of operation are used, 2) to study pyrolysis of a mixture of anaerobically digested sewage sludge (AD-SS) and forest residues (FR) at pilot scale, 3) to evaluate pyrolysis gas quality and identify the fate of impurities from AD-SS and FR feedstock mixtures, specifically with respect to energy recovery applications.

More specifically, to determine if pyrolysis of a mixture of AD-SS + FR could provide a gas of sufficient quality for use in a gas engine with the char offering the potential to be used for combustion.

2. Material and methods

2.1. Material

The anaerobically digested sewage sludge (AD-SS) (waste secondary sludge after anaerobic digestion) was obtained in a form of granular dry material and before pyrolysis it was mixed with forest residues (FR) in a 70/30 ratio by weight (70 % of AD-SS and 30 % FR) and subsequently pelleted. The bulk density of the pellets was 662 kg/m³. The pellets were 1–3 cm long with diameter of 0.5 cm. The proximate and ultimate properties of AD-SS as well as AD-SS and FR mixture are presented in Table 1. The forest residues were used because the two feedstock complement each other and realise a circular economy in industry.

Table 1

Proximate and ultimate properties and chemical composition of AD-SS, mixture of AD-SS with FR as well as chars from laboratory and pilot scale pyrolysis of AD-SS + FR at 800 °C.

Properties, wt. %	FR	AD-SS before pelleting	AD-SS + FR (70/30)	AD-SS + FR Char laboratory	AD-SS + FR Char pilot
Moisture,	18.01	4.86	6.10	1.59	0.57
Ash content, db.	0.29	15.59	13.87	45.91	43.95
Volatile matter, db.	87.01	73.03	74.33	7.28	11.52
Fixed carbon, db.	12.69	11.26	11.92	46.81	44.53
LHV, MJ/kg		14.31	16.36		17.85
C, db.	51.00	46.85	47.36	50.79	48.49
H, db.	6.19	6.16	6.05	0.80	1.50
N, db.	0.28	4.59	4.00	2.85	3.88
S, db.	0.00	0.87	0.76	0.46	0.47
O, db. (by difference)	42.25	25.94	27.96	-0.80	1.71
Lignin, db.		21.62	25.06		
Cellulose, db.		24.86	24.67		
Hemicellulose, db.		6.73	7.65		
Extractives (ethanol), db.		22.32	17.64		

ar. – as received basis.

db. – dry basis.

2.2. Pyrolysis experiments at laboratory scale

Pyrolysis experiments at laboratory scale were performed using a fixed bed reactor described in detail by Agar et al. [50]. The pyrolysis set-up consisted of a quartz tube reactor coupled with a condenser cooler and a twin-neck round-bottom receiving flask where the pyrolysis liquid was collected. The condenser outer jacket was cooled through circulation of a refrigerated liquid at 0 °C. The outlet of the receiving flask was connected to a rubber tube fitted with a connector which enabled gas sampling or connection to a filter (filled with loosely packed paper tissue) for capturing aerosols. The gas leaving the filter was discharged to an extraction hood. The quartz tube reactor was wrapped with a heating tape and high-temperature insulation was wrapped around the outside of the heating tape. An electro-thermal power regulator was used to supply the heating tape with electricity. For each experiment 40 g of AD-SS + FR pellets in a steal-mesh basket was placed in the reactor, heated to 800 °C, and kept at this temperature for 10 min during which the feedstock was pyrolysed. The product gas generated was cooled to room temperature while passing through the cooler. When 20 g of AD-SS + FR pellets were pyrolysed, a sample of gas was collected for compositional analysis. This allowed collection of all generated gas in a 10 L Tedlar bag. When the heating jacket was turned off and the char was cooled to room temperature while still in the reactor. The char yield was obtained as the ratio between mass of the char after pyrolysis and the initial sample mass. The vast majority of pyrolysis liquid was collected in the receiving flask; however, some of the oil/tar condensed on the cool parts of the experimental set-up. Therefore, in order to account for this fraction before and after each series of pyrolysis runs, the reactor with the heating tape and insulation, the receiving flask, the dry condenser, the rubber stopper, the filter and all of the connected glass ware were weighed and the mass of liquid fraction was obtained.

2.3. Pyrolysis experiments at pilot scale

The experimental test was carried out in a pilot scale facility used predominantly for pyrolysis of wood chips at Premier Green Energy, Thurles, Ireland. The pilot facility consists of four main sections: feeding system, pyrolysis reactor with char and gas separation section, gas conditioning section and a gas engine or flare. A detailed description of the facility can be found in [51]. The feedstock residence time in the

retort (pyrolysis reactor) was about 10 min while the residence time of the gas was about 7 s. Pyrolysis gas was mixed with air in the cracking reactor, the residence time of the gas in this reactor was about 3 s. The gas leaving the cracker was conditioned in a water scrubber, activated carbon filter, de-humidifier and finally was reheated before being sent to the flare. A schematic diagram of the experimental facility with sampling points is shown in Fig. 1. Operating process conditions for the pyrolysis experiment for the AD-SS + FR at a steady state operation were as follow: feeding rate 60 kg/h, pyrolysis temperature 800 °C, temperature in the cracking reactor 870 °C and flow rate of air for cracking reactor was 32.2 Nm³/h. For the experiment the following physical properties were measured: mass of feedstock fed in, mass of char produced, volumetric flow of pyrolysis gas and air for the cracking reactor. The gas composition was measured online at the 3rd sampling port while off-line gas samples were collected in Tedlar bags at the 1st and 2nd sampling ports. Samples of gas were taken at all sampling points for determination of solid phase adsorption (SPA) tar content, moisture content and NH₃.

2.4. Heat transfer and conversion efficiency in pyrolysis reactors

The performance of a pyrolysis reactor, product distributions and their properties depend on heat transfer characteristics. The dimensionless *Biot* number *Bi* (Eq. 1) describes the extent of thermal control in the reactor as it is the ratio of heat convection (numerator) and heat conduction (denominator). *Bi* depends on the heat transfer coefficient α ($W m^{-1} K^{-1}$), the particle size r_p (*m*) and the thermal conductivity λ ($W m^{-1} K^{-1}$) of the feedstock.

$$Bi = \frac{\alpha \times r_p}{\lambda} \quad (1)$$

The heat transfer coefficient is calculated (Eq. 2) using reactor-specific specifications for the feedstock heating rate χ ($K s^{-1}$), the feedstock mass *m* (*kg*) and specific heat capacity C_p ($J kg^{-1} K^{-1}$), the surface area *A* (m^2) of the inner reactor wall and the temperature difference ΔT (*K*) between the wall of the reactor and the feedstock (Agar et al. 2018).

$$\alpha = \frac{\chi \times m \times C_p}{A \times \Delta T} \quad (2)$$

The heating rate χ and ΔT are determined experimentally through measuring the reactor wall and feedstock temperature. The area *A* depends on reactor design and geometry.

The specific heat capacity of a two part mixture can be represented (Eq. 3) by a linear combination feedstock heat capacities, where M_1 and M_2 are the mass fraction of the two materials and C_1 and C_2 are their respective heat capacities.

$$C_p = M_1 \times C_1 + M_2 \times C_2 \quad (3)$$

Heat capacities can be approximated as 1950 $J kg^{-1} K^{-1}$ for AD-SS feedstock (C_1) [24] and 1370 $J kg^{-1} K^{-1}$ for forest residues (C_2). A thermal conductivity value of 0.1 $W m^{-1} K^{-1}$ was used in calculations.

The thermal conversion efficiency η_{th} (%) of a pyrolysis process at steady-state conditions can be defined as the ratio of thermal power output *P* (kW) of pyrolysis products (e.g. syngas and char) to the thermal power input P_{feed} (kW) of the feedstock (Eq. 4).

$$\eta_{th} = (P_{gas} + P_{char} + P_{tar}) / P_{feed} \quad (4)$$

P is the product of mass/volume flow and lower heating value (as received) and therefore a function of the moisture content of the feedstock and pyrolysis products.

2.5. Analytical techniques

The pyrolysis gas composition was determined by gas chromatography using an Agilent Micro-GC 3000 equipped with thermal

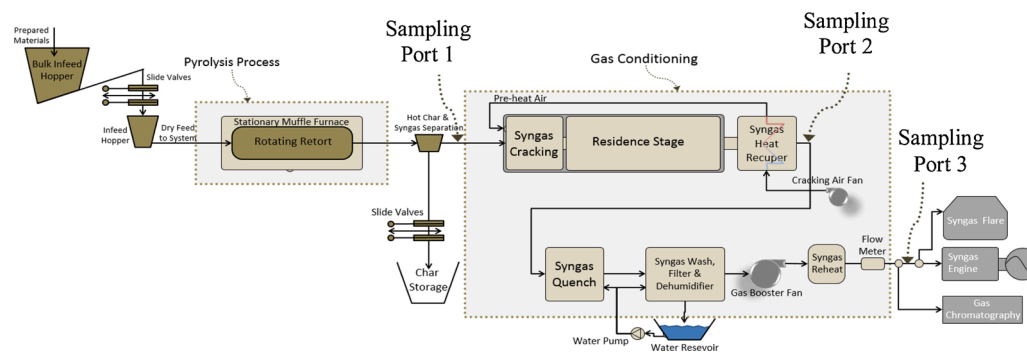


Fig. 1. Schematic diagram of pilot scale facility.

conductivity detectors configured for the detection of CH_4 , CO_2 , C_2H_4 , C_2H_6 , C_2H_2 , H_2S , H_2 , O_2 , N_2 , CH_4 and CO .

The NH_3 content in the pyrolysis gas was measured by means of an off-line quantification procedure, which was applied to the retained amounts of ammonia in absorbing solutions. The NH_3 sampling train consisted of three impingers were filled with 0.8 L of 0.05 M H_2SO_4 solution. A vacuum pump was used to pull the gas through the sampling train. The sampling ports and tubes were insulated in order to avoid water condensation. The ammonia containing samples were steam distilled using Kjeldahl distillation unit, where ammonia was captured by saturated solution of boric acid. The amount of ammonia was determined by back titration with standardised 0.10 M HCl.

Tar samples were taken at three sampling ports. Sampling port 1 was located between the pyrolysis reactor and the thermal tar cracking unit, sampling port 2 was located immediately after the thermal tar cracking unit, and sampling port 3 was just before the internal combustion engine (Fig. 1). The tar sampling ports were designed for the solid phase adsorption (SPA) sampling protocol. 100 mL of the pyrolysis gas was withdrawn by an SPA device comprised of a stainless-steel needle, pre-packed Discovery® DSC- NH_2 SPE cartridge containing amino-propylsilane sorbent, and a 100 mL gas tight syringe. Tar compounds were extracted from the sorbent with $3 \times 600 \mu\text{l}$ of dichloromethane, while tert-butylcyclohexane was added as an internal standard to each extracted tar solution. A gas chromatograph fitted with flame ionization detection (GC-FID) (Thermo Scientific, Model Trace 1310) was employed in order to quantify the tar compounds between 2-methylpropanenitrile and indeno[1,2,3-cd] pyrene. A gas chromatograph coupled with a mass selective detector (GC-MSD) (Agilent 7890A GC and MSD 5975C) was used for identification of the most abundant tar compounds. The calibration of the GC-FID used a single quantitation curve prepared using 5 known concentrations of naphthalene/tert-butylcyclohexane. This simplified calibration, based on a single quantitation curve offers a significant advantage, in terms of speed and quantitation of complex materials such as tar however, it can result in up to 35 % relative expanded uncertainty within the reported results for the GC-FID based measurement system [52]. Total tar yields are referred to as total gas chromatography detectable tar and expressed on a volumetric basis as $\text{g}_{\text{total tar}}/\text{Nm}^3_{\text{dry gas}}$.

Moisture content was determined using an adsorption method. 100 mL of hot gas was drawn through 1.0 g of strong desiccant phosphorus pentoxide (P_2O_5) at 50 mL/min allowing the gas to cool to room temperature (about 25 °C) and achieve complete water adsorption. The moisture content was calculated as the mass gained after adsorption.

Analysis of the ultimate properties of the AD-SS, AD-SS + FR and the pyrolysis char were carried out by Celignis Analytical, Ireland. The elemental composition (C, H, N and S) was determined using a Vario EL cube elemental analyser with oxygen content calculated by the difference. The moisture content was analysed according to BS EN 14774-1: 2009, the ash content according to BS EN 15403: 2011 and the volatile matter content according to the BS EN 15402: 2011 standard procedure.

The proximate and ultimate properties are expressed as weight % (wt. %). The higher heating value (HHV) was measured with a Parr 6300 isoperibolic calorimeter and the corresponding lower heating value (LHV) was calculated.

Analysis of chemical composition of biomass samples was carried out by Celignis Analytical, Ireland. The reader is referred to an earlier publication [53] for a detailed description of the wet-chemical analytical protocol, which is similar to the Uppsala Method [54]. In brief, the samples were extracted with 95 % ethanol using a Dionex Accelerated Solvent Extractor (ASE 200) prior to a two-stage acid hydrolysis to hydrolyse the structural polysaccharides. The liberated monosaccharides were determined using ion chromatography. The acid insoluble residue was dried, weighed, and then ashed to find the Klason lignin (KL) content. All analyses were carried out in duplicate.

Inorganic constituents were measured using inductively coupled plasma optical emission spectrometry (Agilent 5100 ICP-OES fitted with an SPS4 auto-sampler) after nitric acid, hydrogen peroxide and hydrofluoric acid (HNO_3 - H_2O_2 -HF) digestion in a microwave oven according to BS EN 15290:2011. Before digestion AD-SS and AD-SS + FR were ashed at 550 °C.

3. Results and discussion

3.1. Properties of anaerobically digested sewage sludge and mixture with forest residues

In Table 1 the properties of AD-SS, and AD-SS and FR mixture are presented. The ash content of AD-SS was lower while the volatile matter higher compare to AD sewage sludge reported in literature [55]. The nitrogen content was in the range for AD sewage sludge [55–57]. In the AD-SS and FR mixture tested, a volatile matter content of 74.3 wt. % and an ash content of 13.8 wt. % were observed (dry basis). A high volatile matter is advantageous if the pyrolysis gas is a desirable product. A fixed carbon content of 11.9 wt. % indicates the amount of unconverted carbon which potentially will remain in the char after pyrolysis. The nitrogen content was at 4.0 wt. % while a sulphur content of 0.8 wt. %. Mixing of AD-SS with forest residues slightly reduced the ash, nitrogen and sulphur contents in the feedstock. In general, SS and AD sewage sludge contains fibres of lignin, cellulose and hemicellulose as reported by Guo et al. [58]. The chemical composition of AD-SS and AD-SS + FR obtained from wet-chemical analysis is presented in Table 1. The AD-SS sample comprised mainly of cellulose (24.8 wt. %), lignin (21.6 wt. %) and ash (15 wt. %) and small amount of hemicellulose (6.7 wt. %) and ethanol extractives (22.3 wt. %). The content of cellulose is higher while hemicellulose lower compared to [58]. In the AD-SS + FR mixture the content of lignin and hemicellulose increased slightly indicated that its fraction in the FR was higher. On the other hand the content of extractives and ash decreased when compared to the AD-SS sample.

The content of the major and minor elements in the inorganic matter of AD-SS + FR is reported in Table 2 where it can be seen that the silica

Table 2

Content of major and minor ash forming elements in the AD-SS + FR mixture (pellets) and pyrolysis char.

Element	AD-SS + FR mg/kg _{dry} matter	AD-SS + FR char mg/kg _{dry} matter	Increase factor in char, -	Maximum allowable concentration as set by EBC mg/kg _{dry} matter
Al	5558.67	18067.4	3.3	
Ca	17738.78	57044.27	3.2	
Fe	6231.00	19527.47	3.1	
K	1680.48	5403.55	3.2	
Mg	3706.90	11756.57	3.2	
Na	1778.26	5696.83	3.2	
P	12105.93	38443.06	3.2	
S	2998.84	6701.16	2.2	
Si	21656.76	69163.75	3.2	
Ag	35.07	109.72	3.1	
As	0.34	0.00	-	13
Ba	444.40	1474.85	3.3	
Cd	1.35	2.11	1.6	1.5
Co	0.00	0.00	-	
Cr	26.97	97.06	3.6	90
Cu	415.40	1325.04	3.2	100
Hg	0.00	0.00	-	1
Mn	189.49	609.77	3.2	
Mo	7.42	23.21	3.1	
Ni	17.53	69.63	4.0	50
Pb	48.55	162.47	3.3	150
Sb	1.35	0.00	0.0	
Se	0.67	0.00	0.0	
Ti	1061.43	3428.65	3.2	
Sn	22.25	94.95	4.3	
V	8.09	27.43	3.4	
Zn	99.32	3135.37	31.6	400

(21.6 g/kg_{dry} matter) was the most abundant element followed by calcium (17.7 g/kg_{dry} matter) and phosphorus (12.1 g/kg_{dry} matter). The content of iron in AD-SS was about 1/3, aluminium about 1/4, magnesium about 1/6 of that of silica. Among all the heavy metals analysed, the content of Ti was the highest in AD-SS + FR at 1000 mg/kg_{dry} matter followed by Ba and Cu at about 400 mg/kg_{dry} matter. The content of P, Zn, Cu, Ni and Cr in AD-SS + FR was lower than reported for anaerobically digested SS [55,59]. Metal content of sewage sludge ash after incineration was evaluated in Germany [60] and Si, Ca, Fe and Al were among most abundant major elements as well as Zn, Ba, Cu and Mn, Sr, Cr and Pb were found to be most abundant minor elements.

The high amounts of nitrogen and presence of sulphur in the AD-SS bring considerable challenges to its pyrolysis due to the high potential of secondary environmental pollution. During thermal treatment significant amounts of feedstock-bound nitrogen and sulphur are volatilised in the form of NH₃, HCN, and H₂S [25,35] all of which are toxic and/or pollutants. When the pyrolysis gas is combusted these compounds are converted to their respective oxides (i.e. NO_x, N₂O or SO_x) which are contributors to acid rain, greenhouse gas emissions or ozone layer depletion. Moreover H₂S is also corrosive. These compounds need to be removed from the gas in order to avoid corrosion and fouling in the engine.

3.2. Laboratory versus pilot scale experiments

3.2.1. Yield of pyrolysis products

The main aim of the comparison was to quantify the difference in the char yield and the gas composition for pyrolysis test carried out in a simple fixed bed laboratory pyrolysis reactor and rotating retort pyrolyser at pilot scale, when the residence time of the feedstock was 10 min in both cases.

The relative distribution of pyrolysis products was determined by the principle of conservation of mass—the combined mass of pyrolysis products is equal to that of the initial sample feedstock. The experimental uncertainty in the char yield was low because the AD-SS + FR samples and char were measured directly. In contrast the liquid yield

had a greater uncertainty. Even though the whole experimental apparatus was weighed before and after pyrolysis in order to obtain the mass of the liquid fraction there was always some oil condensed in the gas sampling bag. This indicates that some pyrolysis products escaped the apparatus as vapours or aerosols. Thus, based on the conservation of mass, the measured liquid fraction should be considered the minimum. Consequently, as the gas yield is calculated by the difference between the solid and the liquid pyrolysis products and the initial sample mass, the gas yield should be considered the maximum value. The maximum experimental uncertainty in liquid and gas yield was estimated at about 2 %.

The yields of pyrolysis products from laboratory pyrolysis were 27.7, 45.1 and 27.2 wt. % for char, liquid and gas, respectively. The yield of liquid fraction (oil and aqueous, condensable fraction) was the highest among all pyrolysis products. A high yield of liquid product (>40 %) was typical for both slow and fast pyrolysis of anaerobically digested SS as reported by Fonts et al. [55,61] and Inguanzo et al. [62]. The properties of liquid fraction were not further tested in this study, since the residence time for vapours in the laboratory and pilot scale reactor are different (<1 s versus ~7 s) the composition of condensable fraction leaving pilot scale reactor would be different.

The yield of char at 27.7 wt. % was much lower than yields reported for anaerobically digested SS by Inguanzo et al. [62]. In general, the yield of char depends on initial ash content of feedstock, since the ash content in AD-SS + FR was low the char yield was also relatively low.

The yield of gas at 27.2 wt. % was higher than for anaerobically digested SS alone as reported by Inguanzo et al. [62].

The yields of pyrolysis products from pilot scale pyrolysis were 23.4, 33.7 and 42.9 wt. % for char, liquid and gas, respectively. The mass of AD-SS + FR pellets used for the test and char collected were directly measured, and the char yield was calculated. The yield of pyrolysis gas, at port 1 (Fig. 1), was calculated by subtracting the air flow rate for the cracking reactor from the final pyrolysis gas flow rate and converting to the total mass of gas released over the duration of the test. Based on conservation of mass the yield of liquid was calculated as the difference between 100 % and the mass of solid char and gas product. The yield of liquid includes tar yield (measured) as an organic fraction and aqueous fraction which was condensed out in the de-humidifier but not measured directly.

The yield of char from pilot scale was 4 % smaller than that from laboratory scale. Char from pilot scale had much smaller particle size compare to laboratory tests (see Fig. 2). This is due to disintegration of carbonised pellets, whose friability increases with pyrolysis, during mixing in the rotating retort. In the pilot scale system, the extent of thermal decomposition of AD-SS + FR was greater, and the char yield lower, because heat and mass transfer was enhanced through both continuous mixing of feedstock and smaller particle formation; the *Biot* number (Eq. 1) tends to zero as particle radius decreases. The more effective feedstock decomposition/degradation under comparable temperatures highlights the difference between a rotating retort and a fixed bed reactor. Lepez et al. [63] reported a slightly higher char yield of 29 % for SS (100 %) and 41 % for SS mixed with lime for pilot scale pyrolysis at 800 °C in an integrated system of a contact drier and heated worm-screw conveyer reactor (Spirajoule® pyrolyzer, ETIA, France). Though, the higher char yield may be due to higher ash content of SS feedstock compare to AD-SS + FR.

The syngas cracking unit in the pilot-scale system (Fig. 1) and longer residence time of pyrolysis gas in the retort contributed to a lower yield of liquid, as compared to the laboratory reactor, by decomposition of condensable organic molecules (e.g. long hydrocarbon chain condensable gases). This resulted in a liquid yield of only 33.7 % compared to 45.1 % in the laboratory. Therefore, better heat transfer and gas cracking due to a longer residence time in the pilot system enabled 58 % higher conversion of feedstock to gaseous products (i.e. 42.9 vs. 27.2 % in pilot and laboratory, respectively).



Fig. 2. Char from pelleted feedstock in laboratory (left) and pilot scale (right) pyrolysis experiments at 800 °C and residence time of 10 min. The pellet diameter is approximately 5 mm.

3.2.2. Properties of pyrolysis char laboratory versus pilot scale

The proximate and ultimate properties of chars from the laboratory and pilot scale test are presented in Table 1. The main difference between chars is the content of volatile matter, of 7.28 and 11.52 % for laboratory and pilot scale pyrolysis, respectively. Since, at laboratory reactor char was left in the hot reactor to cool down, the release of volatiles continued after the heating was turned off, thus pyrolysis continued after 10 min as the temperature slowly dropped over several minutes but at temperature lower than 700 °C. In contrast at pilot scale char leaving the retort was separated from the gas and collected in an uninsulated vessel (temperature of 200–300 °C), which allow for much faster cooling. In the fixed bed configuration with a prolong contact of vapor-phase pyrolysis species with the char a slightly higher fixed carbon content of the char from laboratory reactor was observed, which is in line with previous findings [64]. The mass balance calculations revealed that 21.0 and 23.8 % of the initial N was retained in the char from laboratory and pilot scale respectively, which is similar to results reported in literature [65]. Regarding S content, after pyrolysis 17.6 and 15.2 % was retained in the char (laboratory and pilot respectively) which is lower than data reported by Zhan et al. [35] who found 50 %, retention of S in the char for sewage sludge pyrolysis. The bulk density of the char from pilot scale was 454.7 kg/m³.

The concentrations of Pb, Cd, Cu, Ni, Zn and Cr in the char from pilot scale pyrolysis exceed the maximum allowable values specified in the European Biochar Certificate [66] (see Table 2).

3.2.3. Pyrolysis gas composition laboratory versus pilot scale

At laboratory scale, the product gas generated was cooled to room temperature while passing through the cooler, and all of it was collected in Tedlar bag. At pilot scale, in order to measure the pyrolysis gas composition prior high temperature conditioning (tar cracking) sample of gas was collected in Tedlar bag from a pipe duct between the pyrolysis reactor and the tar cracking reactor, at gas sampling point 1 (see Fig. 1). Both gas samples were analysed by micro GC. The resulting gas composition on an N₂ and O₂ free basis in Table 3. The calorific value of the untreated pyrolysis gas (Port 1) from pilot tests was higher compare to laboratory scale 26.4 versus 17.4 MJ/m³. The gas from pilot scale contained more CO, CH₄, C₂H₄ and C₂H₆ than gas from laboratory scale, which most likely could be linked with decomposition/cracking of long hydrocarbon chain molecules or steam and dry reforming. Unlike for dairy sludge [51] the concentration of H₂ and CO₂ at pilot scale was very low 0.03 vol. % and 1.4 vol.%, respectively. Lepez et al. [63] reported calorific value of pyrolysis gas, 19.3 MJ/m³, obtained from pilot scale pyrolysis of SS at 800 °C in an integrated system of a contact drier and pyrolyser of Spirajoule® technology. A much higher content of H₂ of 21.4 vol. % was observed in [63] compared to pyrolysis gas derived from AD-SS and FR from both laboratory and pilot scale tests.

Table 3

Composition of pyrolysis gas collected at laboratory and pilot scale. Pyrolysis gas collected before (Port 1) the tar cracker on N₂ and O₂ free basis (pilot scale). Average composition of the pyrolysis gas at steady state operation after conditioning (Port 3) at pilot scale.

Gases, vol. %	Laboratory	Pilot	
		Port 1	Port 3
H ₂	0.8	0.03	1.8 ± 0.9
CO	9.7	45.0	19.0 ± 1.6
CO ₂	15.0	1.4	5.0 ± 1.1
CH ₄	23.8	30.7	9.8 ± 1.3
C ₂ H ₂	0.5	0.1	0.3 ± 0.1
C ₂ H ₄	10.8	12.0	1.3 ± 0.2
C ₂ H ₆	1.2	4.0	0.05 ± 0.1
N ₂	–	–	53.5 ± 2.6
O ₂	–	–	4.4 ± 1.9
H ₂ S, ppm	6449	793	119 ± 45
NH ₃ , g/m ³	–	36.9	0.036
LHV, MJ/m ³	17.4	26.4	7.1 ± 0.7
Total tar, g/Nm ³ dry gas	–	14.6	7.1 ± 0.6
Water content g/Nm ³ dry gas	–	17.5	6.5 ± 7.8
Gas yield, m ³ /h	–	32.3	63.1 ± 1.6
Gas yield, m ³ /kg dry feed	–	0.57	1.1 ± 0.03

3.2.4. Heat transfer and conversion efficiency

The average temperature difference between reactor wall and feedstock (ΔT) and the calculated Biot number a 5 mm particle composed of an AD-SS and FR mixture 70/30 is shown in Fig. 3 for 40 g samples, the heat transfer coefficient α ranged from 0.8 to 3.8 W m⁻² K⁻¹. The heating rate ranged from 92 to 5 K min⁻¹. As the Biot number is the ratio

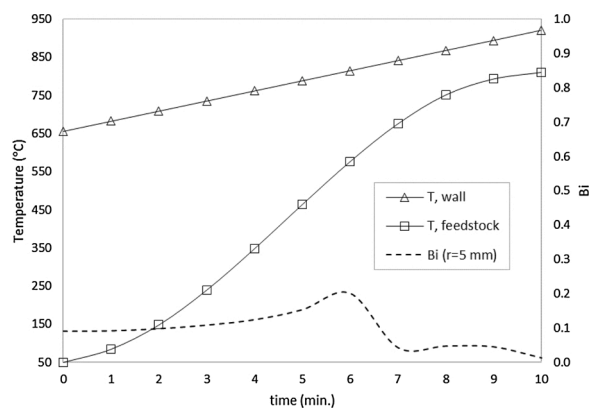


Fig. 3. Modelled temperature profile of laboratory reactor wall and feedstock over the duration of pyrolysis (40 g sample mass). The calculated Biot number (Bi) for 5 mm particle diameters of anaerobically digested sewage sludge and forest residues 70/30 mixture is plotted on the secondary axis.

of heat convection (numerator) and heat conduction (denominator), a value below 1 means that heat transfer within the feedstock is rapid enough for the particles (pellets) to be in thermal equilibrium (i.e. they are uniformly cooked). The relatively small α values in the laboratory reactor lead to a small Biot number (Eq. 1), which has a value below 0.2 indicating that thermal equilibrium exists within the sample and thermal control over the char-forming reactions.

As the pilot scale process uses a rotating retort, is semi-continuous and is combined with gas conditioning, pyrolysis is more dynamic where feedstock within the retort exist at different stages of thermal modification. Determination of local heat transfer coefficients (Eq. 2) are more difficult to define compared to a batch system. These factors combined with the more sophisticated experimental setup makes the pilot scale pyrolysis more difficult to observe and define temperature differentials within the reactor as the feedstock heating rate and residence time cannot be analysed separately. Heat transfer coefficients in rotary kilns with solid feedstock particles (ignoring gas-solid convective heat transfer) are typically between 50 and 100 W m⁻² K⁻¹ [67]. As these values of α are assumed to be valid for the present system, the Biot number (Eq. 1) would be markedly larger than in the laboratory reactor, in the range of 2–5. Therefore, the extent of sample carbonisation may be less homogeneous than in the laboratory case. In the present study, however, comparison of pyrolysis products yield may be a more useful method of comparing heat and mass transfer between the laboratory and pilot scale experiments.

The thermal conversion efficiency (Eq. 4) of the pilot-scale process is estimated at 78 % using the measured moisture content, mass flows and heating values (Table 4). The moisture content of feedstock (6.1 %) was determined from a sample under laboratory conditions. However, the pilot-scale experiment was carried out in winter in an unheated facility when humidity was high and temperature significantly less than room temperature. Therefore, the moisture content of the feedstock was likely much greater as biomass pellets are hydrophilic and their moisture content can easily exceed 10 % when stored in humid conditions at lower temperature [68]. For example, a 10–15 % moisture content would result in a thermal conversion efficiency range of 83–92 %. The difference between this and 100 % can be attributed to combined heat transfer losses in the pilot-scale system (e.g. radiative heat transfer losses from reactor walls and conduits, heat loss from hot char exiting the reactor at 800 °C (Fig. 1), gas cooling and conditioning losses and moisture entering the system in injected air). In a commercial installation, heat transfer losses would be minimised.

3.3. Gas composition from pilot scale after conditioning

The volumetric concentration of the gas components over the run time of the experiment at pilot scale, measured on-line at gas sampling point 3 (before the engine), is shown in Fig. 4 a and b. It can be seen from the figures that the gas composition profiles for the major gas components in Fig. 4a had effectively stabilized after 10 min. In order to ensure steady state had been reached, an additional 10 min were allowed before sampling the product gas for tars and NH₃. The concentration of C₂H₄ however stabilised only around 30 min after the feeding commenced (see Fig. 3b). This could be related to temperature in the cracking reactor, which dropped from 970 to 870 during the first 30 min of the

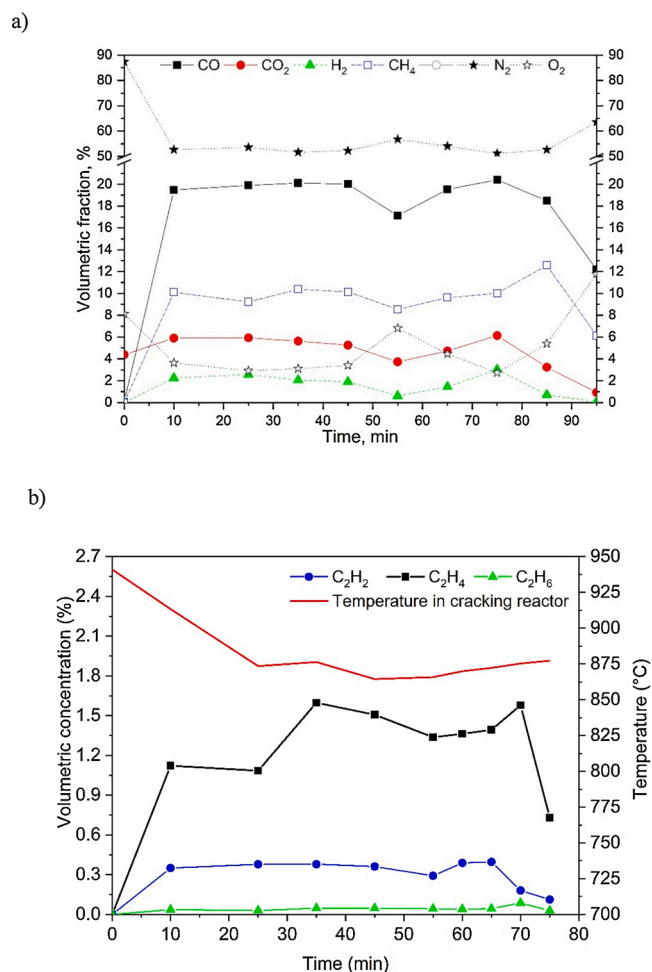


Fig. 4. Content of (a) major and (b) minor gas components in pyrolysis gas after conditioning.

test. The temperature in the cracking reactor was controlled by adjusting the flow of air and it decreased despite the airflow increased from 0.35 to 0.52 Nm³/min. The temperature decrease is most likely linked to the high relative humidity of the air on the day of test.

The average gas composition for steady state operation is presented in Table 3. The calorific value of the conditioned pyrolysis gas 7.1 MJ/m³ (port 3) was lower than that of the raw gas (port 1). Since air was injected into the cracking reactor (see section 2.3), the final gas was diluted with N₂, which accounted for 53.5 vol. %. As the temperature in the cracking reactor was only 80 °C higher than in the pyrolysis reactor, there was no substantial change in the gas composition comparing the concentrations on a N₂ free basis between port 1 and port 3. However, a small increase in CO (from 45.0–47.9 vol. %), H₂ (from 0.03–4.4 vol. %) and C₂H₂ (from 0.1 to 0.8 vol. %) concentration indicate tar transformation. The increase in C₂H₂ is an indicator of tar cracking [69], while in H₂ is a good indicator of reactions that convert primary tars into

Table 4

Measured properties of feedstock and pyrolysis products used to estimate thermal conversion efficiency.

Feedstock		Syngas (port 3)		Char		Tar
MC (%)	6.1	MC (g/Nm ³)	6.5*	MC (%)	0.6	
Mass flow ar (kg/h)	60	Volume flow ar (m ³ /h)		Mass flow ar (kg/h)	14.0	
Mass flow db. (kg/h)	56.3	Volume flow db (m ³ /h)	63.1	Mass flow db. (kg/h)		0.45
LHV db. (MJ/kg)	16.4	LHV db (MJ/m ³)	7.1	LHV db. (MJ/kg)	17.85	
LHV ar (MJ/kg)	14.9	LHV ar (MJ/m ³)		LHV ar (MJ/kg)	17.5	41.14
Power (kW)	248	Power (kW)	124	Power (kW)	64	5

* Moisture in the syngas decreases the LHV ar by only 0.0169 MJ per m³ (0.2 %) and therefore can be neglected.

aromatics, especially polycyclic aromatic hydrocarbons [70]. An increase in CO₂ content (from 1.4–12.5 vol. % on a N₂ free basis) is indicating that effective oxidation of C₂H₄ and C₂H₆ was taking place in the cracking reactor, whose concentration on the other hand significantly decreased (from 12 to 2.6 vol. % and from 4 to 0.1 vol. %, respectively). The present O₂ in the conditioned gas at concentration 4.4 % for the duration of the test, may indicate an ingress of not controlled air or an excess of unreacted oxygen due to too low temperature in the cracking reactor.

3.3.1. Impurities in the pyrolysis gas at pilot scale reactor

3.3.1.1. Tar content and composition. The tar content and composition was measured at the three sampling ports along the pilot scale facility. The results are presented in Table 4. The average total tar yield was reduced between sampling ports 1 and 2, from 14.6 g/Nm³ of dry gas at port 1–8.7 g/Nm³ dry gas at port 2, located after the thermal cracking reactor. Further conditioning of the pyrolysis gas did not have much influence on the tar content measured at port 3, where a value of 7.1 g/Nm³ dry gas was recorded. In the previous section (on gas composition from pilot scale after conditioning) only slight increase in the indicators of tar cracking/aromatisation (C₂H₂ and H₂) was observed, which shows that for this test tar content was reduced only slightly and the decrease in the measured concentration was due to the dilution with air. For comparison for pyrolysis of SS from milk processing factory blended with wood chips [51] the total tar yield was reduced significantly between sampling ports 1 and 2 (from approx. 12 to 3 g/Nm³ dry gas). Further conditioning of the pyrolysis gas did not have much influence on the tar content.

Table 5 shows also the yields of all identified tar compounds denominated according to the IUPAC nomenclature and listed in the order in which they eluted. At the sampling port 1, which corresponds to tar released/formed in the pyrolysis reactor, sixteen N-containing tar species were identified. In Table 5 they are denoted with *. The yields of nitrogen-containing tar compounds account for approx. 12 % of total tar. Pyridine, propenenitrile, 2-methyl-, benzonitrile, and indole are found to be the most abundant N-containing tar compounds. Anzar et al. [65] reported that 16 % of the total N input was released as N-containing tar compounds during gasification of sewage sludge at 725 °C. N-containing compounds were also reported to be present in bio-oil obtained from sewage sludge pyrolysis at 500 °C [55]. These compounds are precursors for N-containing pyrolysis tar whose formation is promoted by increasing pyrolysis temperature and extending the residence time. In the current study, at a pyrolysis temperature of around 800 °C, the tars undergo secondary reforming reactions making their structure less heterocyclic and more aromatic. N-containing tar is considered problematic due to the carcinogenic and mutagenic character of their aromatic analogues [55]. N-containing tar is water soluble, adding organic load to the aqueous liquor which will require treatment. Other identified constituents are well-known pyrolysis tar including aromatic hydrocarbons among which the most abundant ones were: benzene, toluene, styrene, indene, and naphthalene. Along with that O-containing aromatic compounds were represented by cresols, and benzofuran, 7-methyl-. Five S-containing compound were identified (denoted with ** in Table 4). All belonging to aromatic and heterocyclic family of thiophenes making up 1% of total tar. In previous work, when pyrolysing SS from milk factory blended with wood chips the authors identified nine N-containing tar species, while S-containing compounds were rarely present. This is probably due to lower N and S content in the initial feedstock [51].

At a temperature of about 870 °C and in the presence of oxygen, large portion of the N-containing tars were cracked. At port 2 the number of N-containing tar species reduced to four which accounts for only about 1% of total tar. O-containing compounds were all reformed, while three S-containing compound remained present in the pyrolysis gas. As a result

of polymerization trace amount of dibenzothiophene have been measured at the port 2. The yields of total tar sampled at port 3 were expected to be lower compared to those at port 2. It had been anticipated that the water scrubber and activated carbon filter mounted between ports 2 and 3 should have removed a portion of the tar from the pyrolysis gas. Compounds with the mass of indene and heavier did reduce notably. Probably due to condensation effect. In contrary, yields of lighter compounds such as benzene, toluene, and styrene remained constant or as indicated by benzene may even increase. These compounds do not condense at ambient conditions and therefore remain in the pyrolysis gas. Table 5 indicates similar total tar contents for ports 2 and 3.

The calculations indicated that total tar comprises 1.5–2.0 wt. % of the initial weight of dry SS-AD + FR pellets. Dominguez et al. [71] reported a yield of total tar lower than 1 wt. % of the SS feedstock when sampling tar using a wet condensation method.

Tar content could be viewed from two different perspectives, which depend on the final use of the pyrolysis gas. When the hot raw gas is combusted directly such as in boilers or industrial kilns, tars are a source of energy not accounted for in the calorific value of the dry pyrolysis gas. There is little chance of tar condensation and thus there is no need for tar removal and usually no tar limits are specified. The N-containing tars however will release HCN and NH₃ mainly through thermal cracking and during combustion NOx and N₂O will be released. Therefore, de-NOx technology would be required.

However, for use in an internal combustion gas engine tar has to be removed to levels specified by manufacturers. Internal combustion engines require cooled gas, where there is a probability of tar condensation inside the engine or in the fuel-injection systems. In general, tar concentrations in the gas should be well below 100 mg/Nm³ [72] but each manufacturer provides their own specifications. For the Dresser-Rand Group [73] gas engine used in this investigation, gasification or pyrolysis tar limits are specified for tar groups according to the number of aromatic rings. Single aromatic ring tar < 1.5 g/MJ, 2 aromatic rings < 0.2 g/MJ, 3 aromatic rings < 0.003 g/MJ, and no tar compounds with 4 aromatic rings or more are allowed to enter the gas engine. Limits are calculated according to following formula: $limit\ conc. [g\ Nm^{-3}] = specif.\ limit [g\ MJ^{-1}] \times LHV [MJ\ m^{-3}]$. The manufacturer also proposes the CEN/ BT/TF 143 standard technical specification, also known as the tar protocol rather than the SPA method, as a methodology for determination of the tar content in the gas.

Table 5 shows the tar compounds grouped and classified on the basis of number of aromatic rings as measured from sampling ports 1, 2 and 3. Sampling port 1; the limits concerning 1 aromatic ring group are not exceeded whereas 2, 3, and 4+ aromatic rings groups indicates an overstep values. Sampling port 2; thermal tar cracking did reduce 2 aromatic rings group, but the quantities remain on the borderline to manufacturer specifications. On the other hand temperature driven polymerization [72] resulted in higher yields of groups 3 and 4+ aromatic rings. Sampling port 3; water scrubbing together with activated carbon filtration adequately reduced groups of 2 and 3 aromatic rings. But small amount of the most detrimental group of 4+ aromatic rings (i. e. fluoranthrene and pyrene) still remained in the pyrolysis gas. Moreover, the group denominated as an unknown consist of identified non-aromatic tar and unidentified chromatographic peaks. Unknown group is present in amounts that may foul installation and as such should be taken into account.

Given that the tar limits are based on the number of aromatic rings, it suggests that the tar composition is as important as the total tar. Parameters such as tar dew point or selection of a suitable tar removal method will depend on tar composition rather than on total tar. More efficient tar mitigation system is required for optimal performance of a given Dresser-Rand internal combustion gas engine.

3.3.1.2. NH₃ and H₂S. During pyrolysis an attempt was made to quantify the content of NH₃ in the pyrolysis gas. The measured ammonia

Table 5

Yields of individual tar compounds with their chromatographic retention time (a,b,c, and d denote replicate measurements), yields of total GC detectable tar measured by SPA method, as well as the yields of tar groups classified according to the number of aromatic rings.

Tar compounds	Retention time (min)	$\text{g}_{\text{total tar}}/\text{Nm}^3$ dry gas		$\text{g}_{\text{total tar}}/\text{Nm}^3$ dry gas				
		Port 1 a b		Port 2 a b		Port 3 a b		
1	Propenenitrile, 2-methyl-*	2.09	0.33	0.291	–	–	–	–
2	Isobutyronitrile*	2.19	0.127	0.132	–	–	–	–
3	Cyclohexadiene	2.37	0.045	0.041	–	–	–	–
4	1,3-Cyclopentadiene, 5-methyl-	2.46	0.018	0.019	–	–	–	–
5	2-Butenenitrile*	2.63	0.070	0.066	–	–	–	–
6	Benzene	2.70	1.014	1.061	5.416	4.282	6.122	5.722
7	Thiophene**	2.78	0.047	0.048	0.099	0.060	0.069	0.058
8	3-Butenenitrile*	2.90	0.033	0.032	–	–	–	–
9	Butanenitrile, 2-methylene-*	3.86	0.020	0.019	–	–	–	–
10	Pyrazine*	4.01	0.040	0.039	–	–	–	–
11	Pyridine*	4.34	0.416	0.369	0.020	–	–	–
12	Toluene	5.01	2.609	3.222	0.095	0.069	0.082	0.069
13	Thiophene, 2-methyl-**	5.13	0.005	0.006	–	–	–	–
14	Thiophene, 3-methyl-**	5.36	0.028	0.032	–	–	–	–
15	Pyridine, 2-methyl-*	6.94	0.131	0.108	–	–	–	–
16	1H-pyrrole, 2-methyl-*	8.07	0.020	0.016	–	–	–	–
17	Ethylbenzene	8.43	0.301	0.285	–	–	–	–
18	o/m/p-Xylene	8.77	0.582	0.536	–	–	–	–
19	Phenylethyl	9.10	0.012	0.012	0.019	0.010	0.010	0.008
20	Styrene	9.64	1.597	1.432	0.138	0.088	0.080	0.067
21	Pyridine, 3,5-dimethyl-*	11.26	0.061	0.058	–	–	–	–
22	Benzene, propyl-	11.81	0.027	0.025	–	–	–	–
23	Benzene, 1-ethyl 3-methyl-	12.11	0.066	0.058	–	–	–	–
24	Benzene, 1,2,4-trimethyl-	12.34	0.017	0.015	–	–	–	–
25	Benzonitrile*	13.04	0.167	0.176	0.079	0.036	–	–
26	Benzene, 1-ethyl-2-methyl-	13.28	0.508	0.456	–	–	–	–
27	Benzene, 1-propenyl-	14.32	0.049	0.043	–	–	–	–
28	Indene	14.88	0.522	0.479	0.081	0.060	0.006	0.006
29	o/m/p-Cresol	15.77&16.51 16	0.517	0.485	–	–	–	–
30	Benzofuran, 7-methyl-	16.75	0.151	0.153	–	–	–	–
31	Naphthalene, 1,2-dihydro-	18.12	0.185	0.186	–	–	–	–
32	Naphthalene	19.20	1.058	1.038	1.371	1.135	0.026	0.030
33	Benzo(b)thiophene **	19.36	0.054	0.062	0.027	0.042	–	–
34	Quinoline*	20.87	0.110	0.101	–	–	–	–
35	Naphthalene, 2-methyl-	22.26	0.262	0.283	0.009	0.007	–	–
36	Indole*	22.51	0.149	0.214	–	–	–	–
37	Naphthalene, 1-methyl-	22.70	0.208	0.231	0.010	0.006	–	–
38	Naphthalene, 2-ethenyl-	24.50	0.103	0.101	0.036	0.023	–	–
39	Biphenyl	25.74	0.051	0.062	0.012	0.006	–	–
40	Acenaphthylene	26.19	0.113	0.139	0.365	0.230	0.003	0.003
41	Naphthalene 2-carbonitrile*	27.36	0.060	0.074	0.028	0.013	–	–
42	Benzofuran	27.85	–	–	0.008	0.002	–	–
43	Naphthalene 1-carbonitrile*	27.91	0.015	0.023	0.012	0.005	0.004	0.003
44	Fluorene	29.25	0.072	0.091	0.030	0.018	–	–
45	Benzene, 1,1'-(diazomethylene)bis-*	30.30	0.015	0.016	–	–	–	–
46	Dibenzothiophene **	33.10	–	–	0.009	0.005	–	–
47	Anthracene	33.63	0.152	0.227	0.296	0.153	–	–
48	Phenanthrene	33.82	–	–	–	–	–	–
49	1/2-Methylantracene	36.06	0.036	0.051	–	–	–	–
50	4H-Cyclopenta(def)phenanthrene	36.33	–	–	0.023	0.009	–	–
51	Naphthalene, 2-phenyl-	37.50	0.079	0.102	0.009	0.004	–	–
52	Fluoranthrene	39.05&39.50	0.039	0.056	0.162	0.088	0.002	0.001
53	Pyrene	39.97	0.021	0.030	0.172	0.092	0.002	0.002
54	Pyrene, 1-methyl-	41.74	0.016	0.022	–	–	–	–
55	Benzo(ghi)fluoranthrene	44.64	–	–	0.015	0.008	–	–
56	Cyclopenta(cd)pyrene	45.47	–	–	0.046	0.026	–	–
57	Benzo(c)phenanthrene	45.63	0.008	0.010	–	–	–	–
58	Benz(a)anthracene	45.79	0.015	0.022	0.019	0.013	–	–
59	Benz(a)anthracene, 7-methyl-	48.17	0.004	0.006	–	–	–	–
60	Benzo(e)acephenanthrylene	50.34	–	–	–	–	–	–
61	Benzo(e)pyrene	51.31	–	–	0.013	0.007	–	–
62	Benzo(k)fluoranthrene	51.51	0.005	0.007	0.022	0.013	–	–
63	Indeno(1,2,3-cd)pyrene	55.66&56.43	0.003	0.003	0.035	0.019	–	–
	Total GC detectable tar		14.2	15.0	9.4	7.2	7.0	6.5
	Average from all measurements			14.6		8.7	7.1	7.1
	The yields of tars classified according to the number of aromatic rings	Σ 1 ring	8.2	8.5	5.9	4.5	6.4	5.9
		Σ 2 ring	2.9	3.0	1.6	1.3	0.04	0.04
		Σ 3 ring	0.5	0.6	0.7	0.4	0.004	0.005
		Σ 4 ring	0.1	0.2	0.5	0.3	0.004	0.004
		Unknown	2.5	2.7	0.7	0.6	0.6	0.5
	Upper tar limits for Dresser-Rand gas engine: Σ 1 ring 10.6; Σ 2 ring 1.4, Σ 3 ring 0.02 and Σ 4 ring 0 g/Nm ³							

concentrations before gas conditioning was 36.9 g/Nm³ (see Table 3) which accounts for about 41.7 % of the total nitrogen input into the system for the AD-SS and FR mixture (Table 6). This value is higher than reported in the literature, e.g. Wei et al. [74] observed that 16 % of fuel-N converted into NH₃ during pyrolysis of SS while Aznar et al. [65] reported that over 20 % of fuel-N turned into NH₃ during gasification of SS. As much as 34.5 % of the initial N content was not accounted for in the measurements (calculated by subtracting N retained in char, pyrolysis gas and tar at Port 1 from the total initial input of N with AD-SS + FR). This could be an indication that N was present in the form of either HCN or N₂ moreover a part of NH₃ could have been condensing in the lines used during gas sampling because of insufficient insulation. The concentration of HNC was not measured in the current study however it was reported that the fraction of the N released in the form of HNC can be similar to NH₃ [74] or smaller [25,65] depending mainly on heating rate used. On the other hand, it has been reported that during gasification of N-containing SS, up to 44 % of the nitrogen was released as N₂ [65] as a result of catalytic effect of the mineral matter. In the present study it was difficult to distinguish between the N₂ entering the system with air in the interstices between the feedstock particles and N₂ potentially released from the AD-SS and FR pellets. When we consider all the limitation of the current system set-up, a significant amount of the nitrogen input with the feedstock was not accounted for. Around 0.4 % of N was released as nitrogen containing tars at Port 1 and its amount was reduced to 0.02 % at Port 2.

Although, over 92 % of the ammonia was removed from the gas in the water scrubber the NH₃ remaining 46.7 mg/MJ exceeds the recommended limit of 1.5 mg/MJ for Dresser-Rand internal combustion engine. The pilot scale pyrolysis facility used in this case is typically used for testing materials which do not contain high amounts of nitrogen, therefore it is believed that it is possible to improve and optimise the scrubber cleaning section. If, this will not be possible the fraction of FR with the AD-SS needs to be increased in order to further dilute the concentration of NH₃.

An initial sulphur content of 0.76 % was detected in the AD-SS + FR pellets, of which 15.2 % was retained in the char after pyrolysis (Table 6), consequently the balance, 85 %, was released in a gaseous form or as a condensable or water soluble fraction. Only 7.4 % of the initial S input was detected in the gas as H₂S (before water scrubbing) suggesting that about 77.6 % of S input into the system was missing/not measured. The content of H₂S in the conditioned pyrolysis gas was much lower than in the raw gas 119 ppm versus 793 ppm, respectively. Zhan et al. [35] reported about 50 %, retention of S in char for SS pyrolysis and the remaining S was more or less equally distributed between S-gas and S-tar products.

The equivalent concentration of H₂S in the conditioned pyrolysis gas 25.5 mg/MJ is below the maximum permissible limit of H₂S equivalent which is set to 70 mg/MJ for Siemens (Dresser-Rand Group) gas engine.

4. Conclusions

- The result of the study indicate that the slow pyrolysis of a sewage sludge (AD-SS) and forest residue (FR) blended feedstock have potential for energy recovery from these common industrial waste streams. The thermal conversion efficiency of the pilot-scale pyrolysis process, under steady-state conditions, was estimated at 78 % (minimum).
- The yield of char from a rotating retort at pilot scale was 4 % lower than that from a laboratory scale fixed bed reactor. Also, char from pilot scale was of much smaller particle size compared to that from the laboratory tests. Differences in char yield between the two processes could be a result of 1) longer contact time between the pyrolysis gas and char particles in the laboratory reactor (where char-forming reactions are enhanced) and 2) slower cooling of the sample in the laboratory reactor. Better heat transfer and gas cracking due to a longer residence time in the pilot system enabled 58 %

Table 6

Partitioning of nitrogen and sulphur between char, NH₃ and H₂S, N and S-containing tar compounds for pyrolysis of AD-SS with FR at pilot scale. % of N/S not measured represent balance between content of N/S in char and in pyrolysis gas from Port 1 and the initial content in the feedstock.

N content in AD-SS + FR, wt. % dry basis	% of N in char	% of N as NH ₃ Port 1	% of N as tar Port 1	% of N as NH ₃ Port 2	% of N as NH ₃ Port 3	% of N (not measured)
4.0 (100 %)	23.8	41.7	0.4	9.8	0.7	34.1
S content in AD-SS + FR, wt. % dry basis	% of S in char	% of S as H ₂ S Port 1	% of S in tar Port 1	% of S as H ₂ S Port 2	% of S as H ₂ S Port 3	% of S (not measured)
0.76 (100 %)	15.2	7.4	0.3	2.8	2.2	77.1

higher conversion of feedstock to gaseous products (42.9 vs. 27.2 % yield of gas in pilot and laboratory, respectively).

- The blending of AD-SS with FR resulted in beneficial modification of feedstock properties for energy recovery through pyrolysis. (i.e. increased heating value, reduced ash, nitrogen and sulphur contents of feedstock). However, the fraction of FR in the blend needed to exceed 30 % in order to give higher yields of a less contaminated pyrolysis gas.
- A pilot scale pyrolysis of AD-SS (70 %) with FR (30 %) blend produced 574 m³/t of raw pyrolysis gas composed of CO (45 vol. %), CH₄ (30 vol. %) and C₂H₄ (12 vol. %) with a tar content of 14.6 g/Nm³ and NH₃ content of 36.9 g/Nm³.
- Post-pyrolysis treatment of the gas using a cracking reactor (870 °C) with air as the reagent gas followed by treatment in an un-optimized water scrubbing system did not remove sufficient tars and NH₃ to meet the requirements for the Dresser-Rand internal combustion engine in the conditioned pyrolysis gas.
- Considering the complexity of the pilot system, relatively good closure (75–95 %) was observed for the overall mass balance of the process. The carbon balance of the pilot process was found to be good (94 %)

Author statement

Marzena Kwapinska: Conceptualization, Investigation, Formal analysis, Data curation, Validation, Methodology, Resources, Supervision, Visualization, -Writing - original draft, Writing - review&editing. Alen Horvat: Investigation, Data curation, Validation, Methodology, Visualization, Writing - original draft David A. Agar: Conceptualization, Investigation, Data curation, Writing - review&editing James J. Leahy: Resources, Validation, Writing - review&editing, Funding acquisition, Project administration All authors have read and agreed to the published version of the manuscript.

Declaration of Competing Interest

The authors declare that they have no known competing financial interests or personal relationships that could have appeared to influence the work reported in this paper.

Acknowledgment

This work was supported by the Irish State through funding from Science Foundation Ireland (Grant numbers 16/SP/3829, 16/RI3734) and the Environmental Protection Agency (Grant 2016-RE-MS-7).

Appendix A. Supplementary data

Supplementary material related to this article can be found, in the online version, at doi:<https://doi.org/10.1016/j.jaap.2021.105283>.

References

- [1] Irish Water, Dublin, 2014.
- [2] H. Hudcová, J. Vymazal, R. M. Soil Water Res. 14 (2019) 104.
- [3] Fehily Timoney and Company, 1999.
- [4] M.G. Healy, O. Fenton, E. Cummins, R. Clarke, D. Peyton, G. Fleming, D. Wall, L. Morrison, M. Cormican, EPA, ed, 2017. Dublin.
- [5] Q. Chaudhry, L. Castle, Trends Food Sci. Technol. 22 (2011) 595.
- [6] S. Marchesan, M. Prato, ACS Med. Chem. Lett. 4 (2012) 147.
- [7] K. Fijalkowski, A. Rorat, A. Grobelak, M.J. Kacprzak, J. Environ. Manage. 203 (2017) 1126.
- [8] A.M. Mahon, B. O'Connell, M.G. Healy, I. O'Connor, R. Officer, R. Nash, L. Morrison, Environ. Sci. Technol. 51 (2017) 810.
- [9] S.R. Smith, Philosophical transactions of the royal society a: mathematical, Phys. Eng. Sci. 367 (2009) 4005.
- [10] Y. Zeng, S. Zhao, S. Yang, S.-Y. Ding, Curr. Opin. Biotechnol. 27 (2014) 38.
- [11] X.-D. Song, D.-Z. Chen, J. Zhang, X.-H. Dai, Y.-Y. Qi, J. Mater. Cycles Waste Manag. 19 (2017) 332.
- [12] S.S.A. Syed-Hassan, Y. Wang, S. Hu, S. Su, J. Xiang, Renewable Sustainable Energy Rev. 80 (2017) 888.
- [13] M.C. Samolada, A.A. Zabaniotou, Waste Manag. 34 (2014) 411.
- [14] M. Schnell, T. Horst, P. Quicker, J. Environ. Manage. 263 (2020), 110367.
- [15] X. Meng, Q. Huang, J. Xu, H. Gao, J. Yan, Waste Disposal & Sustainable Energy 1 (2019) 99.
- [16] C.A. Salman, S. Schwede, H. Li, E. Thorin, J. Yan, Integrated concept for sludge pyrolysis in waste water treatment plants for biofuel production and nutrients recovery, Sludge Management in Circular Economy, Rome, 2018, pp. 23–25. May.
- [17] S. Werle, Energies 8 (2015) 8562.
- [18] C. Karaca, S. Sözen, D. Orhon, H. Okutan, Waste Manag. 78 (2018) 217.
- [19] Z. Mei, D. Chen, J. Zhang, L. Yin, Z. Huang, Q. Xin, Waste Manag. 106 (2020) 77.
- [20] A. Zielińska, P. Oleszczuk, B. Charnas, J. Skubiszewska-Zięba, S. Pasieczna-Patkowska, J. Anal. Appl. Pyrolysis 112 (2015) 201.
- [21] D. Chen, L. Yin, H. Wang, P. He, Waste Manag. 34 (2014) 2466.
- [22] F. Mandl, Statistical Physic, Wiley, 1991 p.
- [23] E. Alakangas, in, 2005.
- [24] Y. Kim, W. Parker, Bioresour. Technol. 99 (2008) 1409.
- [25] F.-J. Tian, B.-Q. Li, Y. Chen, C.-Z. Li, Fuel 81 (2002) 2203.
- [26] K. Ericsson, L.J. Nilsson, Biomass Bioenergy 30 (2006) 1.
- [27] P. Lehtikangas, Biomass Bioenergy 20 (2001) 351.
- [28] N. Walker, M. Bazilian, P. Buckley, Biomass Bioenergy 33 (2009) 1229.
- [29] R. Sathre, L. Gustavsson, Biomass Bioenergy 35 (2011) 2506.
- [30] G. Guest, F. Cherubini, A.H. Strømman, Mitig. Adapt. Strateg. Glob. Chang. 18 (2013) 1089.
- [31] L. Shen, D.-K. Zhang, Fuel 82 (2003) 465.
- [32] M.R. Stambach, B. Kraaz, R. Hagenbucher, W. Richarz, Energy Fuels 3 (1989) 255.
- [33] I. Fonts, A. Juan, G. Gea, M.B. Murillo, J.L. Sánchez, Ind. Eng. Chem. Res. 47 (2008) 5376.
- [34] J. Solar, I. de Marco, B.M. Caballero, A. Lopez-Urionabarrenechea, N. Rodriguez, I. Agirre, A. Adrados, Biomass Bioenergy 95 (2016) 416.
- [35] J. Zhang, W. Zuo, Y. Tian, L. Chen, L. Yin, J. Zhang, Environ. Sci. Technol. 51 (2017) 709.
- [36] J.M. Johansen, J.G. Jakobsen, F.J. Frandsen, P. Glarborg, Energy Fuels 25 (2011) 4961.
- [37] K.-M. Hansson, J. Samuelsson, C. Tullin, L.-E. Åmand, Combust. Flame 137 (2004) 265.
- [38] H. Lu, W. Zhang, S. Wang, L. Zhuang, Y. Yang, R. Qiu, J. Anal. Appl. Pyrolysis 102 (2013) 137.
- [39] M. Waqas, S. Khan, H. Qing, B.J. Reid, C. Chao, Chemosphere 105 (2014) 53.
- [40] F. Chen, Y. Hu, X. Dou, D. Chen, X. Dai, J. Anal. Appl. Pyrolysis 116 (2015) 152.
- [41] V. Frišták, M. Pipíška, G. Soja, J. Clean. Prod. 172 (2018) 1772.
- [42] H.-j. Huang, T. Yang, F.-y. Lai, G.-q. Wu, J. Anal. Appl. Pyrolysis 125 (2017) 61.
- [43] Z. Wang, L. Xie, K. Liu, J. Wang, H. Zhu, Q. Song, X. Shu, Waste Manag. 89 (2019) 430.
- [44] Z. Wang, X. Shu, H. Zhu, L. Xie, S. Cheng, Y. Zhang, Environ. Technol. 41 (2020) 1347.
- [45] B. Zhao, X. Xu, S. Xu, X. Chen, H. Li, F. Zeng, Bioresour. Technol. 243 (2017) 375.
- [46] M. Kończak, P. Oleszczuk, J. Hazard. Mater. 400 (2020), 123144.
- [47] P. Manara, A. Zabaniotou, Renewable Sustainable Energy Rev. 16 (2012) 2566.
- [48] M. Kończak, P. Oleszczuk, K. Różyto, J. Co2 Util. 29 (2019) 20.
- [49] J. Jin, M. Wang, Y. Cao, S. Wu, P. Liang, Y. Li, J. Zhang, J. Zhang, M.H. Wong, S. Shan, P. Christie, Bioresour. Technol. 228 (2017) 218.
- [50] D.A. Agar, M. Kwapinska, J.J. Leahy, Environ. Sci. Pollut. Res. - Int. (2018).
- [51] M. Kwapinska, A. Horvat, Y. Liu, J.J. Leahy, Waste Biomass Valorization 11 (2020) 2887.
- [52] A. Horvat, M. Kwapinska, G. Xue, S. Dooley, W. Kwapinski, J.J. Leahy, Energy Fuels 30 (2016) 2187.
- [53] D.J. Hayes, Bioresource Technology, 2012, p. 393.
- [54] O. Theander, P. Aman, E. Westerlund, R. Andersson, D. Pettersson, J. AOAC Int. 78 (1995) 1030.
- [55] I. Fonts, M. Azuara, G. Gea, M.B. Murillo, J. Anal. Appl. Pyrolysis 85 (2009) 184.
- [56] L.E. Sommers, J. Environ. Qual. 6 (1977) 225.
- [57] H. Kominko, K. Gorazda, Z. Wzorek, Waste Biomass Valorization 8 (2017) 1781.
- [58] H. Guo, J.B. van Lier, M. de Kreuk, Water Res. 173 (2020), 115617.
- [59] W.A. Ramírez, X. Domene, O. Ortiz, J.M. Alcañiz, Bioresour. Technol. 99 (2008) 7168.
- [60] O. Krüger, A. Grabner, C. Adam, Environ. Sci. Technol. 48 (2014) 11811.
- [61] I. Fonts, G. Gea, M. Azuara, J. Ábrego, J. Arauzo, Renewable Sustainable Energy Rev. 16 (2012) 2781.
- [62] M. Inguanzo, A. Domínguez, J.A. Menéndez, C.G. Blanco, J.J. Pis, J. Anal. Appl. Pyrolysis 63 (2002) 209.
- [63] O. Lepez, A. Grochowska, A. Malinowski, P. Stolarek, S. Ledakowicz, Thermal Treatment of Sewage Sludge by Integrated Processes of Drying and Pyrolysis in a Pilot Bench Scale, European Meeting on Chemical Industry and Environment, Tarragona, 2015, pp. 10–12. June.
- [64] L. Wang, Ø. Skreiberg, M. Gronli, G.P. Specht, M.J. Antal, Energy Fuels 27 (2013) 2146.
- [65] M. Aznar, M.S. Anselmo, J.J. Manyà, M.B. Murillo, Energy Fuels 23 (2009) 3236.
- [66] E.B.F. EBC, Arbaz, Switzerland, 2012.
- [67] A. Funke, R. Grandl, M. Ernst, N. Dahmen, Chem. Eng. Process. Process. Intensif. 130 (2018) 67.
- [68] T. Järvinen, D. Agar, Fuel 129 (2014) 330.
- [69] G. Taralas, V. Vassilatos, K. Sjorstrom, D. J. Can. J. Chem. Eng. 69 (1991) 1413.
- [70] P. Morf, P. Hasler, T. Nussbaumer, Fuel 81 (2002) 843.
- [71] A. Domínguez, J.A. Menéndez, M. Inguanzo, J.J. Pis, Bioresour. Technol. 97 (2006) 1185.
- [72] T.A. Milne, R.J. Evans, National Renewable Energy Laboratory, Golden, Colorado, US, 1998.
- [73] Dresser-Rand, 2016.
- [74] L. Wei, L. Wen, T. Yang, N. Zhang, Energy Fuels 29 (2015) 5088.